Article

Discovery Medicine 2025; 37(201): 2269–2282
https://doi.org/10.24976/Discov.Med.202537201.193

Mechanisms of Allicin Improving Immunotherapy in Non-Small Cell Lung Cancer by Modulating KDM5B/SETDB1 Axis

Cheng Chen[1,*,†], Weina Li[1,†], Yiling Jiang[1], Guofei Ren[2], Hongjin Yu[1], Jing Fang[1]

[1]Department of Medical Oncology, Affiliated Xiaoshan Hospital, Hangzhou Normal University, 311202 Hangzhou, Zhejiang, China
[2]Department of Pharmacy, Affiliated Xiaoshan Hospital, Hangzhou Normal University, 311202 Hangzhou, Zhejiang, China
*Correspondence: chencheng8588@126.com (Cheng Chen)
[†]These authors contributed equally.
Submitted: 30 June 2025 Revised: 22 August 2025 Accepted: 2 September 2025 Published: 20 October 2025

Background: Allicin has demonstrated promoting effects on the sensitivity of non-small cell lung cancer (NSCLC) cells to radiotherapy. Herein, we further explore the mechanism by which allicin improves NSCLC immunotherapy.
Methods: NSCLC cells were subjected to different concentrations of allicin, where protein levels of lysine demethylase 5B (KDM5B) and SET domain bifurcated histone lysine methyltransferase 1 (SETDB1) were measured. To unveil the mechanism of allicin, KDM5B overexpression plasmid and short hairpin RNA for SETDB1 (shSETDB1) were first constructed, and transfected into cells. The basic function and molecular expressions of NSCLC cells were examined. *In vivo* studies were performed through constructing hormonal tumour mice model. After administration of allicin and/or anti-programmed death receptor 1 (PD-1), changes in tumour growth, KDM5B and SETDB1 expressions, and immune cell infiltration were analyzed by tumour volume measurement, differentiation assays, immunohistochemical staining, and flow cytometry.
Results: Allicin down-regulated KDM5B and SETDB1 protein expressions in NSCLC cells ($p < 0.05$). Allicin inhibited NSCLC cell viability, migration and invasion, while promoting apoptosis ($p < 0.05$). Overexpression of KDM5B counteracted the therapeutic effect of allicin, while shSETDB1 reversed the effect of KDM5B ($p < 0.05$). *In vivo*, allicin significantly inhibited the growth of transplanted tumours, repressed the expressions of KDM5B and SETDB1, promoted CD8+ T-cell infiltration and reduced the proportion of tumour-associated macrophages (TAM) in the tumour ($p < 0.05$). With the addition of anti-PD-1 therapy, allicin showed synergistic adjuvant effects ($p < 0.05$).
Conclusion: Allicin inhibits the malignant function of NSCLC cells by regulating KDM5B/SETDB1 and potentiates the suppressing effect of anti-PD-1 therapy on tumour growth.

Keywords: immunotherapy; allicin; lysine demethylase 5B; SETDB1; PD-1

Introduction

Lung cancer is a leading cause of cancer-related deaths worldwide, with a significant age-dependent increase in incidence [1]. According to the data from the Institute of Cancer Research of the Chinese Academy of Medical Sciences, an estimated 1,060,600 new cases of lung cancer in China in 2022 are projected, with mortality reaching up to 733,300 [2]. Notably, non-small cell lung cancer (NSCLC) represents the main pathological type of lung cancer, accounting for about 85% of the cases [3]. Currently, the treatment of NSCLC is still based on different pathological stages and molecular types. For example, patients in early stages I to III typically undergo surgery, while patients in advanced stages unsuitable for surgical resection receive individualized radiotherapy after evaluation and staging [4]. Since 2015, immunotherapy represented by immune checkpoint inhibitors (ICIs) has transformed the treatment paradigm of NSCLC in different settings and has undergone rapid development [5,6]. ICIs have evolved into a promising therapeutic approach from backline to first-line, from monotherapy to combination, and from late-stage to early-stage.

The immune system functions in three main phases, elimination, homeostasis and evasion [7]: immune effector cells kill tumour cells through cytotoxic mechanisms, while tumour cells with less immunogenic phenotypes are able to evade this elimination and, over time, produce tumour cells that allow their hosts to develop immune-evasion capabilities. During the development of malignant tumours, anti-tumour immunity remains suppressed. The main mechanism of ICIs involves deregulating T-cell suppression to activate the anti-tumour immune response [8,9], and activating other cells of the innate and adaptive immune system, which synergistically promote effective anti-tumour immune responses. Besides, ICIs are widely used in clinical practice, including antibodies against cytotoxic T-

lymphocyte associated antigen 4 (CTLA-4), programmed death receptor 1 (PD-1) and the ligand PD-L1 [9]. The PD-1/PD-L1 immune checkpoint is one of the main evasion mechanisms for tumour cells. PD-1 is expressed on T cells as a co-inhibitory signal, and its interaction with PD-L1 expressed by tumour cells or antigen-presenting cells effectively inhibits T cell activation, reduces cytokine production, and even induces apoptosis of T cells, allowing tumours to evade immune surveillance [10,11]. However, due to the natural immunosuppressive characteristics of malignant tumours, only a small number of patients can benefit from ICIs in the long term, and most patients may develop drug resistance within a certain period of time. Concurrently, the enhanced immune system may also lead to an imbalance in the body's immunity, with activated effector T cells attacking normal tissues, producing autoantibodies, generating substantial cytokines, and inducing autoimmune inflammation, which in turn generates immune-related adverse events (iRAEs) [8,12]. Therefore, developing a safer, more effective adjuvant therapy to improve the efficacy of ICIs is urgently needed.

Allicin is a general term for a variety of sulphur-containing compounds in garlic, which is generated from broken garlic tissues by enzymatic reaction in the natural state. Compared with many chemically synthesised substances, allicin shows advantages including non-toxicity in humans and animals, non-resistance to drugs, environmental compatibility, and low cost [13]. The alliinase enzyme hydrolyzes and cleaves alliin, yielding dehydroalanine and the highly labile allyl sulfenic acid, which rapidly dimerizes to form allicin at ambient temperature [14]. By dint of structural properties, allicin can quickly pass through cell membranes to reach the cells and increase bioavailability. Studies have shown that allicin has a wide range of anti-tumour functions [14,15]. Allicin can act on cancer cells through the mitochondrial apoptosis pathway, and can also inhibit the invasion and metastasis of cancer cells directly, limiting their proliferation. With further research, the suppressing effect of allicin on cancer cell proliferation resorts to autophagic death, important protein signalling, death receptor apoptosis signalling and some key oncogenes [14,15]. Allicin also has an antipathogenic effect against bacteria, viruses, fungi, and parasites, which can increase the gut's normal flora (beneficial bacteria), reducing immune system burden [14]. Beyond its direct antibacterial effects, allicin restores immune homeostasis during UTIs via targeting MALT1/NF-κB signaling [16]. Our prior research revealed [17] that allicin enhances the sensitivity of A549 cells to X-rays by targeting lysine demethylase 5B (KDM5B) through upregulation of miR-486-5p.

A recent study pointed out [18] that KDM5B inhibits reverse transcription factors by recruiting SET domain bifurcated histone lysine methyltransferase 1 (SETDB1), thereby promoting immune evasion. KDM5B is an epigenetic enzyme of the Jumonji C domain-containing (JMJD) family with histone demethylation function. The expression of KDM5B is restricted in normal adult tissues. However, elevated levels of KDM5B have been found in a variety of human cancers. It is considered a transcriptional repressor and is associated with tumour growth, angiogenesis, invasion, metastasis, DNA damage repair and chemotherapy resistance in cancer [19]. SETDB1 acts as a histone methyltransferase capable of catalysing methylation modifications on the Histone H3 Lysine 9 (H3K9) [20], and modulating chromatin openness and the binding of transcription factors to chromatin, thereby impacting gene expression. Therefore, this study aims to explore whether allicin may improve the immunotherapeutic efficacy of NSCLC by regulating the KDM5B/SETDB1 axis.

Materials and Methods

Cell-Related Basic Treatments

Culture

The human NSCLC cell lines A549 (AW-CELLS-CH0021) and H1299 cells (No. AW-CELLS-CH0241) were supplied by Shanghai AnWei-sci Biotechnology Co., Ltd. (Shanghai, China). The basal medium of A549 cells was prepared using Ham's F-12K medium (PM150910A, Wuhan Pricella Biotechnology Co., Ltd., Wuhan, China), and that of H1299 cells was 1640 basal medium (PM150113A, Wuhan Pricella Biotechnology Co., Ltd., Wuhan, China). In order to provide growth conditions, the complete media were all configured with 10% fetal bovine serum (F8687, Sigma-Aldrich, St. Louis, MO, USA). The incubation was performed in 37 °C cell incubator with 5% CO_2. All cell lines were validated by STR profiling and tested negative for mycoplasma.

Overexpression/Knockdown Plasmid Construction and Transfection

The group commissioned Yunzhou Biosciences (Guangzhou) Co., Ltd. (China) to construct KDM5B overexpression plasmid (vector name: pRP[Exp]-CMV>hKDM5B [NM_001314042.1]) and short hairpin RNA of SETDB1 (shSETDB; vector name: pRP[shRNA]-U6>hSETDB1[shRNA#1]; target sequence: CCCGAGGCTTTGCTCTTAAAT), as well as their negative controls (NC corresponds to overexpressed KDM5B, shNC corresponds to shSETDB, 5′CCTAAGGTTAAGTCGCCCTCG3′). CDS region of KDM5B can be found in **Supplementary Material**. According to the grouping (Control (Con), NC, KDM5B, shNC, and shSETDB1 groups), liquid A (5 µg NC/KDM5B overexpression plasmid/shNC/shSETDB+125 µL reduced serum medium) and liquid B (10 µL Lipofectamine 3000 reagent+125 µL reduced serum medium) were prepared 5 min in advance, and then fully mixed (15 min). The plasmids were transfected into cells, followed by quantitative real-time polymerase chain reaction (qRT-PCR) to detect the transfection efficiency after 48 h.

Intervention of Allicin

Firstly, allicin (purity: 98%, HY-N0315, MedChemExpress, Monmouth Junction, NJ, USA) was prepared into a concentration of 10 mg/mL with DMSO. During drug treatment, the allicin at concentrations of 0, 10, 20, and 40 μg/mL was added to the cell culture medium. A549 or H1299 cells in the Con group were normally cultured, while those in the Allicin-10/20/40 groups were incubated with 10, 20 or 40 μg/mL allicin for 72 h, respectively. Based on the results of the previous experiments, allicin at the concentration of 40 μg/mL was selected for our *in vitro* experiments. Specifically, after normal cell culture, the culture medium was changed, and cell culture medium containing 40 μg/mL allicin was used to culture transfected/untransfected A549 or H1299 cells for 72 h.

Grouping

A549 or H1299 cells were assigned into shNC+NC (transfection of shNC and NC plasmids), Allicin+shNC+NC, Allicin+shNC+KDM5B, and Allicin+shSETDB1+KDM5B groups. In the last three groups, before 72-h treatment with cell culture medium containing 40 μg/mL allicin, A549 or H1299 cells were transfected with shNC+NC plasmids, shNC+KDM5B overexpression plasmids, and shSETDB1+KDM5B overexpression plasmids, respectively.

Cell Counting Kit-8 (CCK-8) Assay

A549 or H1299 cells were inoculated in 96-well plates (5×10^4 cells/well). After transfection or allicin treatment, 10 μL/well of CCK-8 solution (K1018, APExBIO Technology LLC, Houston, TX, USA) was added to the cell culture medium. After 4-h culture, optical density at 450 nm was detected using SpectraMax iD5 Microplate Readers (Molecular Devices, San Jose, CA, USA). Cell viability was determined as follows:

Cell viability (%) = $(OD_{Experimental} - OD_{blank}) / (OD_{Control} - OD_{blank}) \times 100$.

Detection of Apoptosis

Allicin-treated A549 or H1299 cells were resuspended by PBS. Apoptosis was detected using the Annexin V-FITC/PI Apoptosis Kit (E-CK-A211, Elabscience Biotechnology Co., Ltd., Wuhan, China). Specifically, cells (5×10^5 cells/well) collected after centrifugation were diluted by 500 μL 1× Annexin V Binding Buffer. Subsequently, 5 μL of Annexin V-FITC Reagent and 5 μL of PI Reagent were added to the A549 or H1299 cell suspensions, which were gently mixed and incubated for 15 min away from light. Later, the samples were transferred to a BECKMAN COULTER flow cytometer (CytoFLEX, Beckman Coulter, Inc., Brea, CA, USA) for apoptosis detection.

Transwell Assay

A 24-well transwell chamber (8.0 μm; 3422, Corning Incorporated, Corning, NY, USA) was used to assay the migration and invasion of NSCLC cells. Matrigel gel (only for invasion assay; 356231, Corning Incorporated, Corning, NY, USA) and serum-free medium at a ratio of 1:8 were spread flat on the transwell upper chamber and waited for solidification. Base medium was added to the upper chamber of the transwell, and complete medium containing 10% FBS was added to the lower chamber. Pre-treated A549 or H1299 cells were inoculated in the upper chamber. After 24 h of incubation, cells in the lower chamber were collected and fixed. Cells undergoing crystal violet staining were observed under a microscope (magnification: 200×; BX-51, OLYMPUS, Hachioji, Tokyo, Japan) for counting.

Basic Animal-Related Handling

Fifty-four C57BL/6 mice (male; 6–8 weeks, 19–22 g) were purchased from Hangzhou Medical College for animal studies, and were reared in a habitable environment with free access to food. The animal experiments were approved by the Ethics Committee of Zhejiang Baiyue Biotech Co., Ltd. for Experimental Animals Welfare (No. ZJBYLA-IACUC-20230915), and the pain of the mice was minimised.

Construction of the Tumour Xenograft Model and Drug Treatment

To construct a humanized xenograft model for NSCLC, transfected/untransfected H1299 cells (5×10^5 cells/mouse, suspended in 200 μL phosphate buffered saline (PBS) (C0221A, Beyotime, Shanghai, China)) were injected subcutaneously into the right axilla of NOD-*scid IL2rγ*^{null} (NSG) mice reconstituted with human immune system (NSG HIS) [21]. The volume of the tumour was measured every 7 days (volume = (length × width^2) / 2). Referring to previous literature [22], 3.5 mg/kg (Allicin-L) and 7 mg/kg (Allicin-H) of allicin were selected, and were administered to model mice by gavage (2 days/dose). Programmed cell death protein 1 (PD-1) treatment is a recognised method [21]. When the tumour volume reached 50 mm^3, InVivoMab anti-human PD-1 (200 μg/mouse; BE0188, BioXcell, Lebanon, NH, USA) was injected into mice via intraperitoneal injection (every 3 days starting 1 day before tumour cell inoculation) [23].

Grouping

In the first part of the animal experiments, the groups are as follows:

(1) Con group: Six mice were injected with untransfected H1299 cells;

(2) Allicin-L group: Six mice were injected with untransfected H1299 cells and then received 3.5 mg/kg of allicin treatment by gavage;

(3) Allicin-H group: Six mice were injected with untransfected H1299 cells and then received 7 mg/kg of allicin treatment by gavage.

In the second part of the experiment, the groups are as follows:

(1) Vector group: Six mice were injected with H1299 cells transfected with NC plasmid;

(2) Vector+PD-1 group: Six mice were injected with H1299 cells transfected with NC plasmid and then treated with anti-PD-1;

(3) Vector+PD-1+Allicin group: Six mice were injected with H1299 cells transfected with NC plasmid and then treated with anti-PD-1 and 7 mg/kg allicin;

(4) KDM5B+PD-1 group: Six mice were injected with H1299 cells transfected with the KDM5B overexpression plasmid and then treated with anti-PD-1;

(5) KDM5B+Allicin group: Six mice were injected with H1299 cells transfected with the KDM5B overexpression plasmid and then treated with 7 mg/kg allicin;

(6) KDM5B+PD-1+Allicin group: Six mice were injected with H1299 cells transfected with the KDM5B overexpression plasmid and then treated with anti-PD-1 and 7 mg/kg allicin.

Immunohistochemical Staining

To reduce the pain of mice, mice were anaesthetised using 3% isoflurane (R510-22-10, RWD, Shenzhen, China) on day 21 and euthanized by dislocating his cervical spine. Subsequently, the intact tumours in mice were surgically excised and weighed. Some tumour tissues were made into paraffin-embedded sections. After dewaxing and hydration, the sections were immersed in Citrate Antigen Retrieval Solution (P0081, Beyotime, Shanghai, China), and incubated with Bovine Serum Albumin (BSA) Blocking Buffer (SW3015, Solarbio, Beijing, China) for 30 min to seal the non-specific binding sites. Then, the sections were incubated with diluted anti-CD8 antibody (1:2000, ab217344, Abcam, Cambridge, UK) overnight, and with Goat Anti-Rabbit Immunoglobulin G (IgG) Heavy & Light chains (H&L) (1:500, ab150077, Abcam, Cambridge, UK) for 30 min. Colour development was accomplished using the Diaminobenzidine (DAB) Horseradish Peroxidase Colour Development Kit (P0202, Beyotime, Shanghai, China). Sections were placed under a microscope (magnification: 100×, Carl Zeiss AG, Zeiss LSM 900, Jena, Germany) to observe the positive expression of CD8 (brown colour). CD8-positive rate was determined as follows:

CD8-positive rate (%) = (Number of positive cells / Number of total cells) × 100.

Detection of the Proportion of Immune Cells in the Tumour

Flow cytometry was used in the study to analyze the proportion of CD8+ T cells and tumour-associated macrophages (TAM) in the tumour. Stripped transplanted tumours were clipped and digested into single cell suspensions [24]. After centrifugation, the cells were resuspended in PBS (1×10^6 cells/mL), and subsequently incubated with the following fluorescently labelled antibodies (Abcam, Cambridge, UK): Fluorescein Isothiocyanate (FITC) Anti-CD8 alpha antibody [EPR21769] (1:500, ab237367), Alexa Fluor® 647 Anti-CD4 antibody [EPR20122] (1:500, ab252150), PE Anti-F4/80 antibody [EPR20548] (1:100, ab237335), and APC Anti-CD11b antibody [M1/70] (1:500, ab25482). Next, the ratio of CD8+ T cells (screening criteria: CD4-CD8+) and tumour-associated macrophages (TAM; screening criteria: CD11b+F4/80+) was determined using CytoFLEX flow cytometer (Beckman Coulter, Inc., Brea, CA, USA). The gating strategy was established using negative control tubes (unstained cells or isotype-matched controls). Positive populations were defined as events exceeding the 99th percentile of fluorescence intensity in the negative control. Fluorescence minus one (FMO) controls were employed to compensate for spectral overlap in multicolor panels.

Table 1. Primers for qRT-PCR.

Primers		Primer sequence (5′ to 3′)
KDM5B (mouse)	F	ATCGCTTGCTGCACCGTTAT
	R	CGCTCATCATCTGGCAACAG
KDM5B (human)	F	CAACTCGGACTTGCTGTTGC
	R	TTCTGGCTTCCGTTGTCTCC
SETDB1 (mouse)	F	CATTTGCCGGCCACTGAAAA
	R	GCAAGCTGGCTTTCCAAGTC
SETDB1 (human)	F	CTATATGACTTCCGGCGGATGA
	R	GCATTGTCCGAAGGCAGAGA
GAPDH (mouse)	F	GAGAAACCTGCCAAGTATGATGAC
	R	AGAGTGGGAGTTGCTGTTGAAG
GAPDH (human)	F	GGAGCGAGATCCCTCCAAAAT
	R	GGCTGTTGTCATACTTCTCATGG

qRT-PCR, quantitative real-time polymerase chain reaction; *KDM5B*, lysine demethylase 5B; *SETDB1*, SET domain bifurcated histone lysine methyltransferase 1; *GAPDH*, glyceraldehyde-3-phosphate dehydrogenase; F, forward; R, reverse.

Quantitative Real-Time Polymerase Chain Reaction (qRT-PCR)

Total RNA from cells (A549, H1299) or tissues (mouse tumours) was isolated by TRIzol RNA Extraction Reagent (R0016, Beyotime, Shanghai, China). Total RNA was reversely transcribed to cDNA following the instructions of the Golden 1st cDNA Synthesis Kit (with dsNase; D0401, HaiGene, Harbin, China). The qRT-PCR assay system was composed of pre-synthesised primers (relevant information is listed in Table 1), cDNA, RAPA3G SYBR Green qPCR Mix (A2250-00, HaiGene, Harbin, China) and diethyl pyrocarbonate (DEPC) water. The reagents to be detected were added to the ABI 7500fast Real-Time PCR

Table 2. Antibodies used in western blot.

Antibodies	Dilution rate	Molecular weight	Production No.
KDM5B	1/2000	165 kDa	ab181089, Abcam, Cambridge, UK
SETDB1	1/2000	158 kDa	ab12317, Abcam, Cambridge, UK
SETDB1	1/1000	158 kDa	ab313862, Abcam, Cambridge, UK
GAPDH	1/5000	34 kDa	ab8245, Abcam, Cambridge, UK
Goat anti-rabbit IgG H&L	1/5000	—	ab6721, Abcam, Cambridge, UK
Goat anti-mouse IgG H&L	1/5000	—	ab150113, Abcam, Cambridge, UK

IgG, Immunoglobulin G; H&L, Heavy & Light chains.

System and the CT value of each gene was obtained. Relative mRNA levels were calculated based on the $2^{-\Delta\Delta CT}$ formula. Conventional glyceraldehyde-3-phosphate dehydrogenase (*GAPDH*) genes were selected for the internal reference.

Western Blot

Lysates (R0010, Solarbio, Beijing, China) were added to cells (A549, H1299) or tissues (mouse tumours) to isolate the total proteins. Protein concentration was then detected using a bicinchoninic acid (BCA) kit (PC0020, Solarbio, Beijing, China). The denatured proteins were added to a pre-configured sodium dodecyl sulfate polyacrylamide gel electrophoresis (SDS-PAGE), followed by an electrophoresis-electrotransfer treatment to complete the separation and transfer of proteins. Following polyvinylidene fluoride (PVDF) membrane sealing, the membrane was sequentially immersed in diluted primary and secondary antibodies (relevant information is listed in Table 2). The antigen-antibody complexes were presented as bands in the gel imager (Tanon 3500, Tanon Science & Technology Co., Ltd., Shanghai, China) after the enhanced chemiluminescence (ECL) luminescent solution was added dropwise. Relative protein level = grey value of target protein / grey value of internal reference protein (GAPDH).

Statistical Analysis

The study was statistically analyzed using GraphPad Prism 8.0 software. Data were expressed as mean ± standard deviation. One-way analysis of variance (ANOVA) analysis was used for comparison between multiple groups (Dunnett post hoc test was used for comparisons between Fig. 1B,C,E,F, Fig. 5A–C,E,F and Fig. 6; Tukey post hoc test was used for comparisons between the rest figures). Two-way ANOVA was employed for the analyses in Fig. 5A and Fig. 7A. Results were considered statistically significant at $p < 0.05$.

Results

Allicin Inhibited the Expressions of KDM5B and SETDB1 in NSCLC Cells

After A549 and H1299 cells were treated with different concentrations of allicin, we detected the levels of KDM5B and SETDB1 proteins. The results showed that medium (20 µg/mL) and high (40 µg/mL) concentrations of allicin could effectively inhibit the protein expressions of KDM5B and SETDB1 ($p < 0.05$, Fig. 1A–F), of which 40 µg/mL allicin had the most remarkable effect (Fig. 1A–F). Therefore, the subsequent cell treatment selected 40 µg/mL allicin. After construction of the overexpression/knockdown plasmids, we first tested the transfection efficiency. As shown in Fig. 1G–J, KDM5B overexpression plasmids substantially up-regulated the mRNA level of *KDM5B* ($p < 0.05$, Fig. 1G,H), while shSETDB1 significantly suppressed the expression of *SETDB1* ($p < 0.05$, Fig. 1I,J).

Allicin Regulated the Malignant Function of NSCLC Cells by Decreasing the KDM5B/SETDB1 Expression

In cell function experiments, we first demonstrated that allicin inhibited the viability of A549 and H1299 cells ($p < 0.05$, Fig. 2A,B), promoted apoptosis ($p < 0.05$, Fig. 2C–F), and reduced migration ($p < 0.05$, Fig. 3A,B,D,F) and invasion ($p < 0.05$, Fig. 3A,C,E,F). However, after KDM5B overexpression, the effects of allicin were counteracted, as evidenced by enhanced cell viability ($p < 0.05$, Fig. 2A,B), reduced apoptosis ($p < 0.05$, Fig. 2C–F), and apparently increased migration and invasion ($p < 0.05$, Fig. 3). Moreover, shSETDB1 reversed the effect of KDM5B overexpression. We found that the viability of A549 and H1299 cells was reduced ($p < 0.05$, Fig. 2A,B), migration and invasion were inhibited ($p < 0.05$, Fig. 3), and the proportion of apoptosis was significantly increased in the presence of shSETDB1 ($p < 0.05$, Fig. 2C–F). We subsequently detected changes in KDM5B and SETDB1 protein expressions using western blot. Similarly, allicin decreased the protein levels of KDM5B and SETDB1 ($p < 0.05$, Fig. 4A–F). When KDM5B was overexpressed, the downregulated levels of KDM5B and SETDB1 were reversed ($p < 0.05$, Fig. 4A–F). When SETDB1 was knocked down, the expression level of KDM5B was unchanged, yet SETDB1 protein expression was suppressed ($p < 0.05$, Fig. 4A–F).

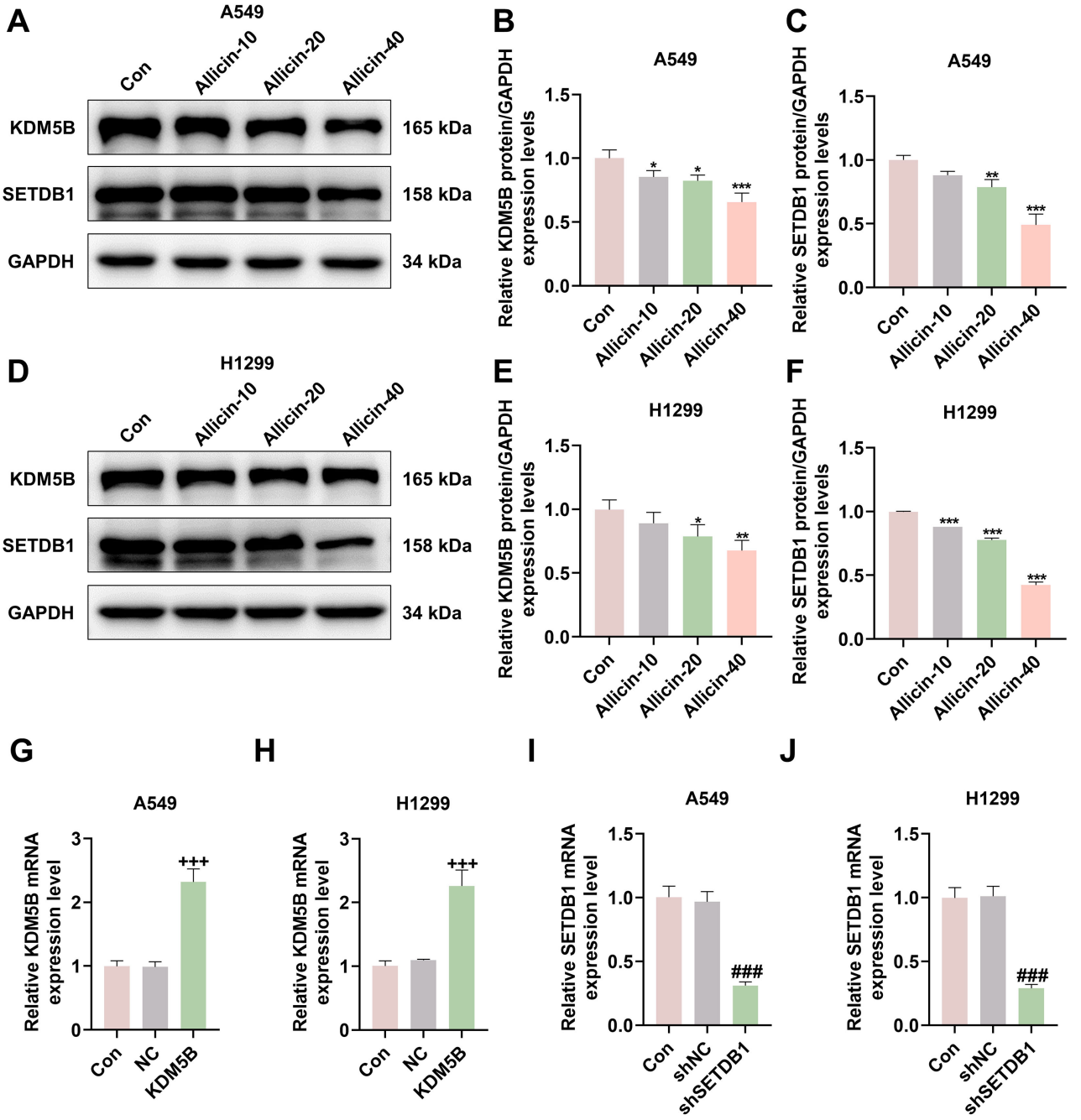

Fig. 1. Allicin inhibited the expressions of KDM5B and SETDB1 in NSCLC cells. (A–F) The effects of different concentrations of allicin on KDM5B and SETDB1 protein expressions in NSCLC cells were detected by western blot. (G,H) Transfection efficiency of KDM5B overexpression plasmid was determined by qRT-PCR. (I,J) Transfection efficiency of shSETDB1 was tested by qRT-PCR. GAPDH was the internal reference gene. All experiments were repeated three times to average. $^{*}p < 0.05$, $^{**}p < 0.01$, $^{***}p < 0.001$ vs. Con; $^{+++}p < 0.001$ vs. NC; $^{###}p < 0.001$ vs. shNC. Abbreviations: NSCLC, non-small cell lung cancer; KDM5B, lysine demethylase 5B; SETDB1, SET domain bifurcated histone lysine methyltransferase 1; NC, KDM5B overexpression negative control for plasmid; shSETDB1, short hairpin RNA for SETDB1; shNC, negative control for shSETDB1.

Allicin Inhibited the Growth of Transplanted Tumours and Reduced CD8+ T-Cell Damage

In animal experiments, transplanted tumour mice were constructed and received allicin treatment. On day 14, we found that allicin treatment evidently inhibited the growth of transplanted tumours ($p < 0.05$, Fig. 5A). Furthermore, allicin markedly waned the expressions of KDM5B and SETDB1 in the transplanted tumour ($p < 0.05$, Fig. 5B–F). In line with the immunohistochemical results, the area of brown positive expression was increased in the allicin-H

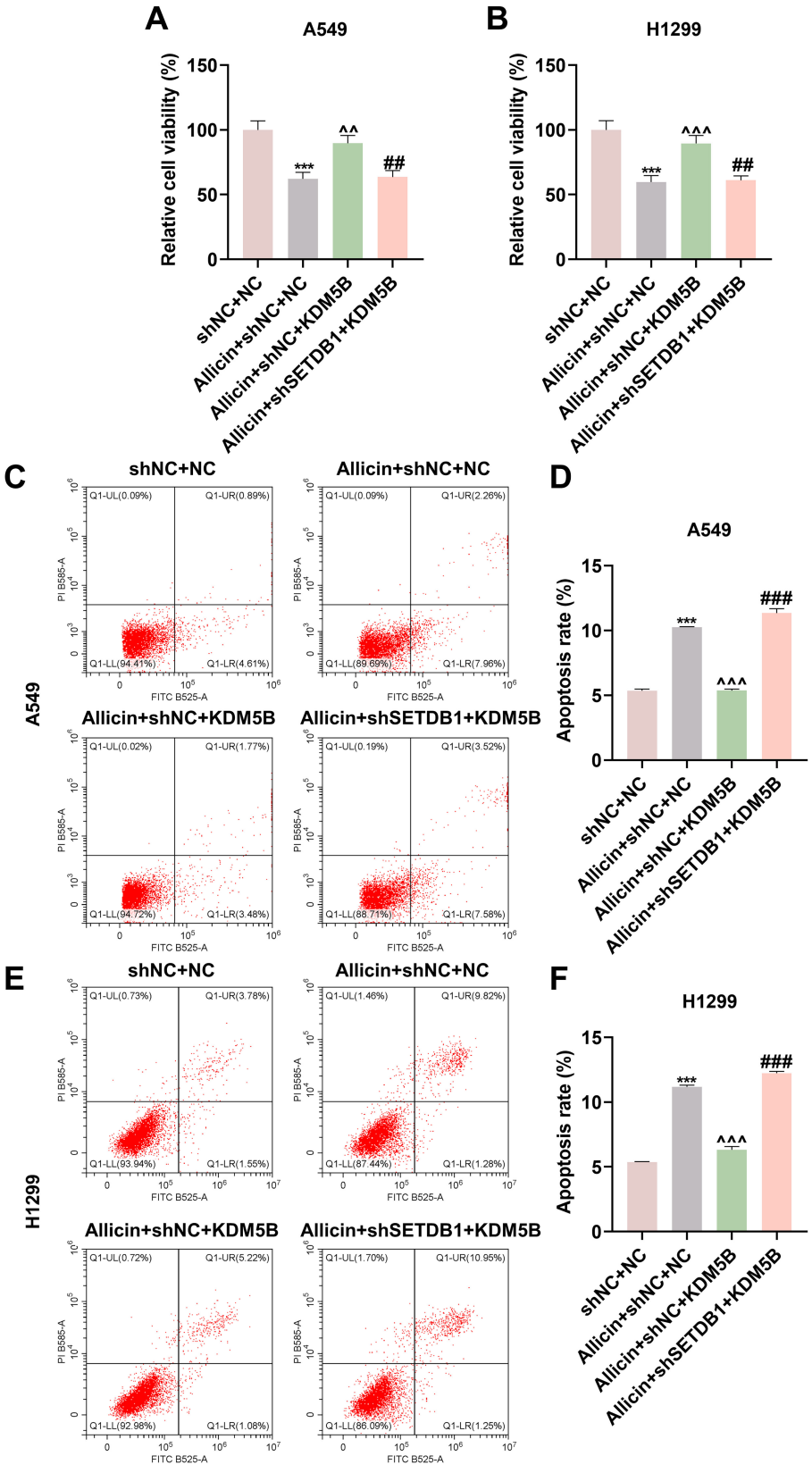

Fig. 2. Effects of allicin, KDM5B, and SETDB1 on NSCLC cell viability and apoptosis. (A,B) Cell viability was measured by cell counting kit 8 assay in A549 cells (A) and H1299 cells (B). (C–F) Apoptosis was examined by flow cytometry in A549 cells (C,D) and H1299 cells (E,F). All experiments were repeated three times to average. $^{***}p < 0.001$ vs. shNC+NC; $^{\wedge\wedge}p < 0.01$, $^{\wedge\wedge\wedge}p < 0.001$ vs. Allicin+shNC+NC; $^{\#\#}p < 0.01$, $^{\#\#\#}p < 0.001$ vs. Allicin+shNC+KDM5B.

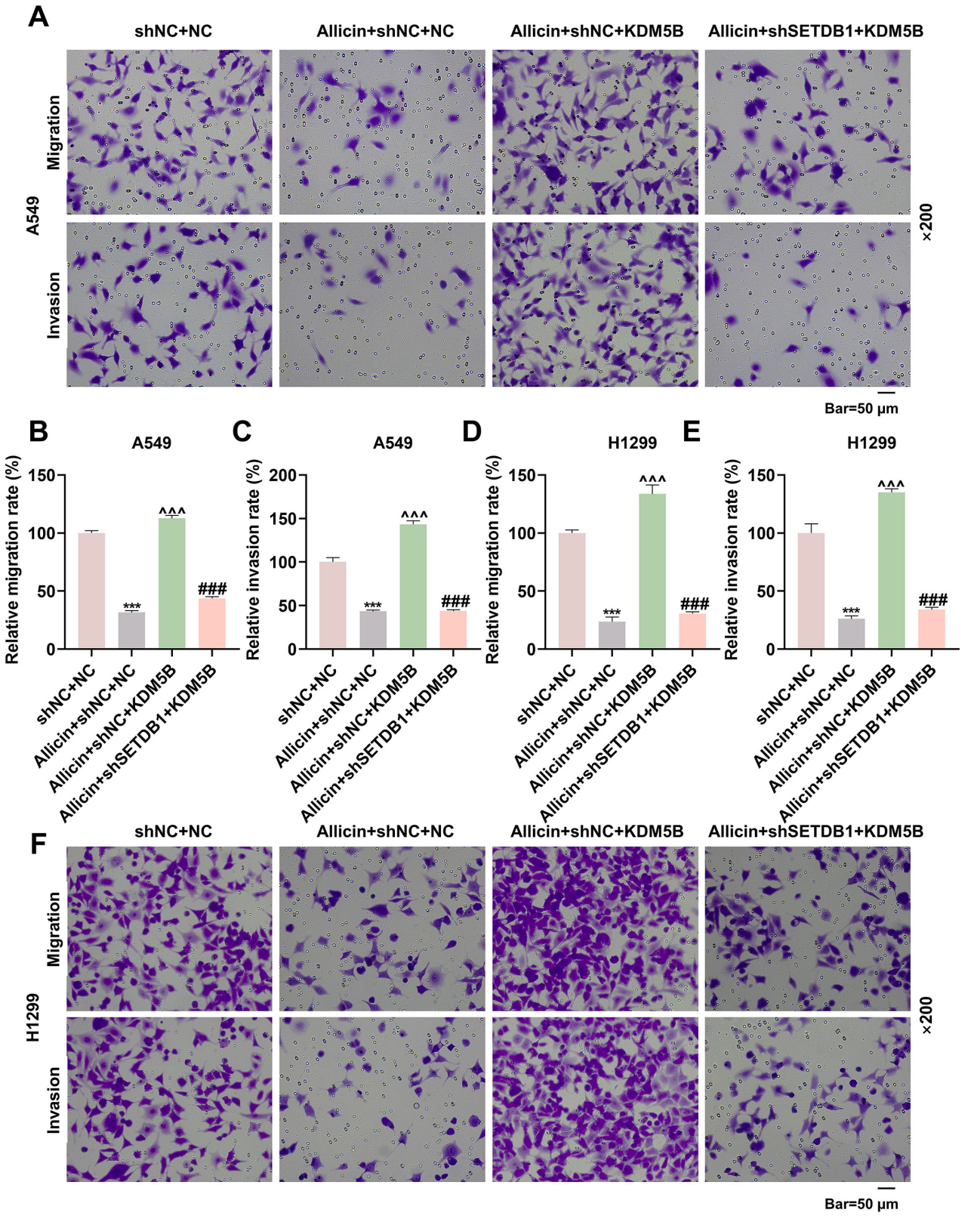

Fig. 3. Effects of allicin, KDM5B, and SETDB1 on NSCLC cell migration and invasion. (A–F) Cell migration and invasion were detected by Transwell assay in A549 cells (A–C) and H1299 cells (D–F) Magnification: 200×. All experiments were repeated three times to average. $^{***}p < 0.001$ vs. shNC+NC; $^{\wedge\wedge\wedge}p < 0.001$ vs. Allicin+shNC+NC; $^{\#\#\#}p < 0.001$ vs. Allicin+shNC+KDM5B.

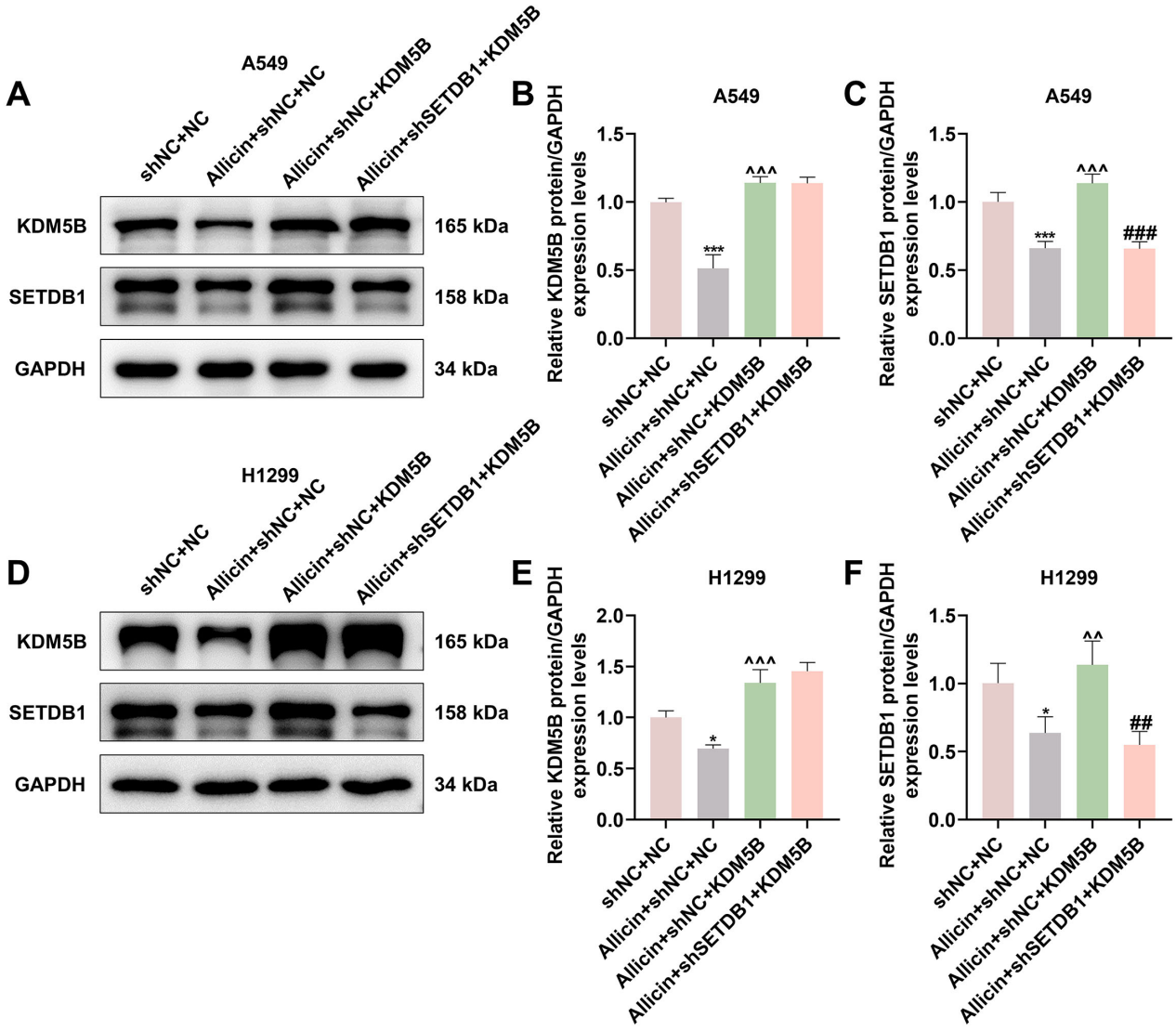

Fig. 4. The changes of KDM5B/SETDB1 axis in NSCLC cells. (A–F) The effects of allicin, KDM5B and SETDB1 on KDM5B/SETDB1 expression in NSCLC cells were examined by western blot. GAPDH was the internal reference. All experiments were repeated three times to average. $^{*}p < 0.05$, $^{***}p < 0.001$ vs. shNC+NC; $^{\wedge\wedge}p < 0.01$, $^{\wedge\wedge\wedge}p < 0.001$ vs. Allicin+shNC+NC; $^{\#\#}p < 0.01$, $^{\#\#\#}p < 0.001$ vs. Allicin+shNC+KDM5B.

group compared with the Con group ($p < 0.05$, Fig. 6A,B), hinting that allicin might positively impact CD8 T cell. We further detected the infiltration of CD8+ T cells and TAM within the tumour using flow cytometry. The results showed that allicin effectively increased CD8+ T cell infiltration and decreased the proportion of TAM ($p < 0.05$, Fig. 6C–F).

Allicin Enhanced the Anti-Tumour Effect of Anti-PD-1 by Modulating KDM5B

In the next animal experiment, we supplemented anti-PD-1 immunotherapy. From day 14, anti-PD-1 treatment exhibited stable tumour growth-inhibiting effects (Vector+PD-1 vs. Vector; $p < 0.05$, Fig. 7A), while allicin played an adjuvant therapeutic role and further dampened the growth of tumour volume (Vector+PD-1+Allicin vs. Vector+PD-1; $p < 0.05$, Fig. 7A). However, the adjuvant effect of allicin was reversed due to overexpression of KDM5B (KDM5B+PD-1+Allicin vs. Vector+PD-1+Allicin; $p < 0.05$, Fig. 7A). Immunohistochemical staining results revealed (Fig. 7B,C) that there was a trend of increased positive expression of CD8 in the Vector+PD-1+Allicin group compared with the Vector+PD-1 group ($p < 0.05$); however, the expression of CD8 was signally reduced in the tumours of the KDM5B+PD-1+Allicin group compared with the Vector+PD-1+Allicin group ($p < 0.05$). Immunocyte infiltration assay data unveiled that anti-PD-1 treatment increased CD8+ T cell infiltration and decreased the proportion of TAM (Vector+PD-1 vs. Vector; $p < 0.05$, Fig. 7D–G), which was strengthened by additional

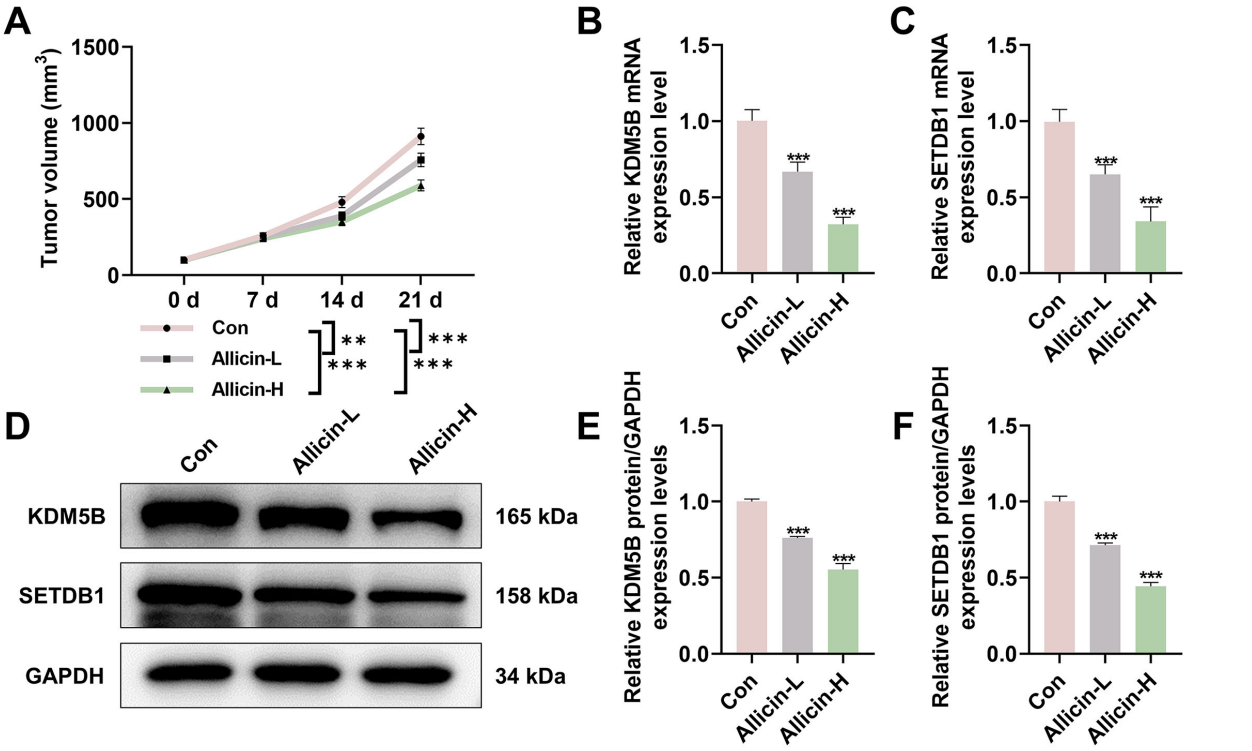

Fig. 5. Allicin inhibited transplanted tumour growth. (A) The effect of allicin on transplanted tumour growth was examined by measuring the volume. (B–F) The effects of allicin on the expressions of KDM5B and SETDB1 in transplanted tumours were detected by qRT-PCR (B,C) and western blot (D–F). GAPDH was the internal reference. All experiments were repeated three times to average. $^{**}p < 0.01$, $^{***}p < 0.001$ vs. Con. Abbreviations: Allicin-L, mice treated with 3.5 mg/kg of allicin; Allicin-H, mice treated with 7 mg/kg of allicin; TAM, tumour-associated macrophage.

allicin treatment (Vector+PD-1+Allicin vs. Vector+PD-1; $p < 0.05$, Fig. 7D–G). Similarly, after overexpression of KDM5B, such effect of allicin treatment was offset, as demonstrated by decreased number of CD8+ T cells and increased proportion of TAM infiltration (KDM5B+PD-1+Allicin vs. Vector+PD-1+Allicin; $p < 0.05$, Fig. 7D–G).

Discussion

In the past decade, PD-1/PD-L1 inhibitors have evolved rapidly, reshaping the landscape of NSCLC treatment and becoming the first-line standard of care for advanced NSCLC [25,26]. Despite its improving effects on prognosis, only a minority of NSCLC patients derive benefit from PD-1/PD-L1 inhibitors [27,28], with drug resistance and adverse effects remaining key impediments to efficacy. Therefore, numerous immunotherapy adjuvants are being actively developed. Building upon our prior finding that allicin enhances NSCLC radiosensitivity [17], through the follow-up experiments, we confirmed that allicin could potentiate the effect of anti-PD-1 immunotherapy.

In addition, we explored the adjuvant mechanism of allicin and unraveled that the KDM5B/SETDB1 axis is involved in adjuvant therapeutic effects of allicin. In NSCLC, KDM5B has been shown to promote tumour invasiveness by activating multiple related biological processes through c-Met signalling, thereby contributive to the poor prognosis [29]. There is a paucity of studies regarding KDM5B and immune regulation, most of which focus on the body's immune-inflammatory response [30,31]. However, recent research firstly linked KDM5B with tumour immune escape, demonstrating that KDM5B inhibits endogenous reverse transcription factors in melanoma cells by recruiting SETDB1 [18]. KDM5B is a key epigenetic regulator in NSCLC, with its high expression associated with tumour aggressiveness and poor prognosis [29], based on which we demonstrated for the first time that by inhibiting KDM5B signalling, allicin improves the efficacy of anti-PD-1 therapy against NSCLC transplanted tumours. KDM5B inhibition might theoretically trigger compensatory upregulation of other histone-modifying enzymes (e.g., KDM5A, HDACs) to maintain tumour survival. Concretely, KDM5B inhibition may upregulate KDM5A or related members to preserve H3K4 methylation homeostasis, while loss of its demethylase activity can trigger compensatory upregulation of co-repressor components (e.g., HDACs) to maintain transcriptional repression [32]. Future studies should employ epigenetic inhibitor screening or proteomic analyses to comprehensively evaluate potential escape mechanisms.

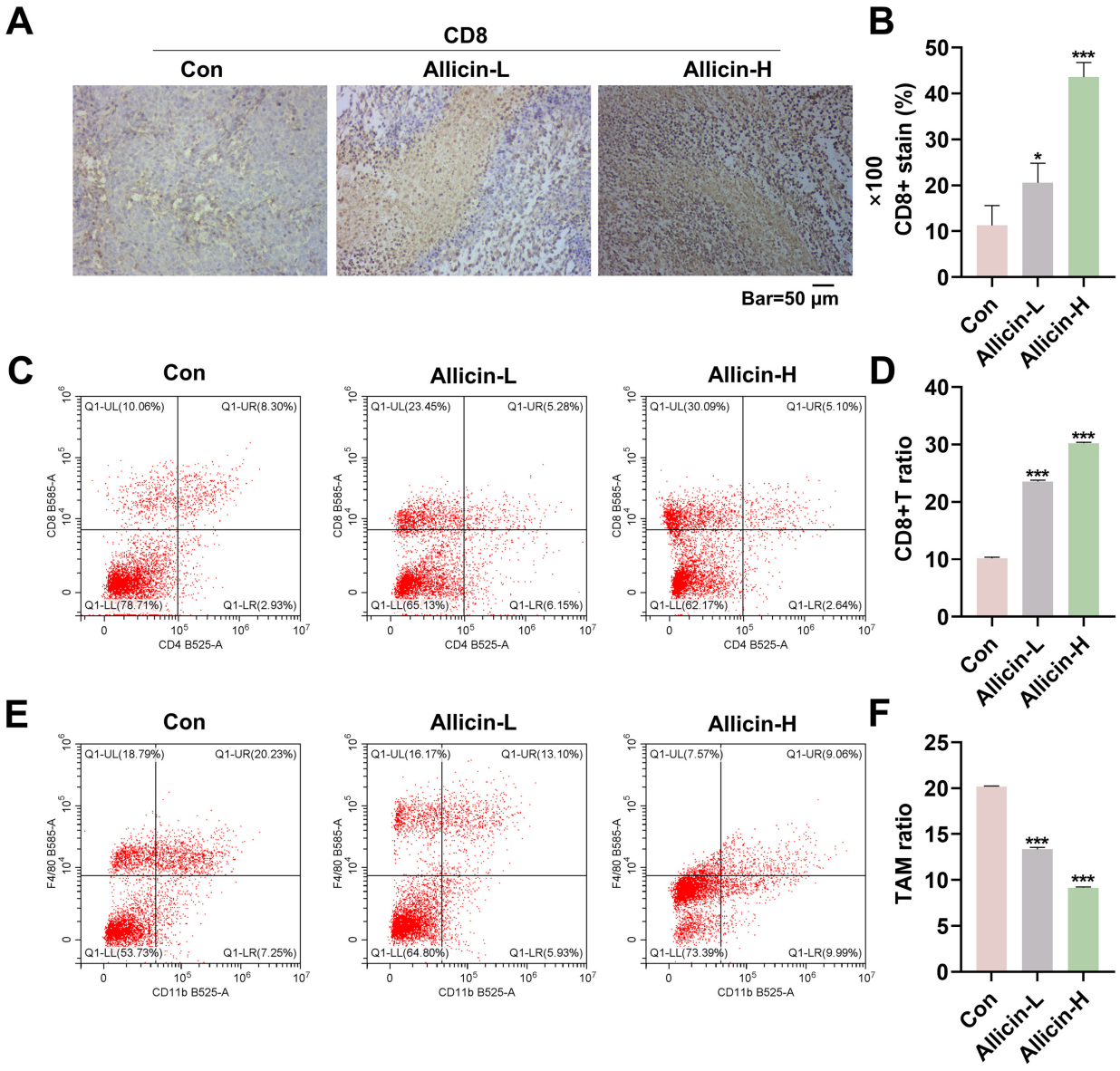

Fig. 6. Allicin reduced CD8+ T cell damage. (A,B) The effect of allicin on CD8 expression in transplanted tumours was observed by immunohistochemical staining. Magnification: 100×. (C–F) The effect of allicin on CD8+ T cells and TAM infiltration in transplanted tumours was detected by flow cytometry. All experiments were repeated three times to average. $^{*}p < 0.05$, $^{***}p < 0.001$ vs. Con. Abbreviations: Allicin-L, mice treated with 3.5 mg/kg of allicin; Allicin-H, mice treated with 7 mg/kg of allicin; TAM, tumour-associated macrophage.

Studies have shown that SETDB1 amplification is strongly associated with tumour immune rejection and anti-immune checkpoint blockade [33,34], and has therefore been identified as an epigenetic checkpoint that suppresses intrinsic tumour immunogenicity [34]. Our study further revealed that KDM5B promotes immune evasion in NSCLC through recruiting H3K9 methyltransferase SETDB1, suggesting its dual role in both tumour progression and immunosuppression. Regrettably, our study only demonstrated an inhibitory effect of allicin on SETDB1 expression without analyzing downstream immune escape mechanisms. Moreover, a previous study demonstrated that in biological systems, allicin can traverse cellular compartments, where it reacts rapidly with free thiol groups to exert biological and pharmacological effects [14]; however, whether or how this reaction also occurs in the medium needs further study. Notably, our study is the first to link Allicin-mediated KDM5B inhibition to SETDB1-dependent immune activation in NSCLC, a mechanism distinct from prior melanoma studies.

Nonetheless, there are some limitations in this study. Firstly, the blood concentration and bioavailability of allicin have not been measured in the animals, and its low tissue accumulation may limit therapeutic efficacy in patients,

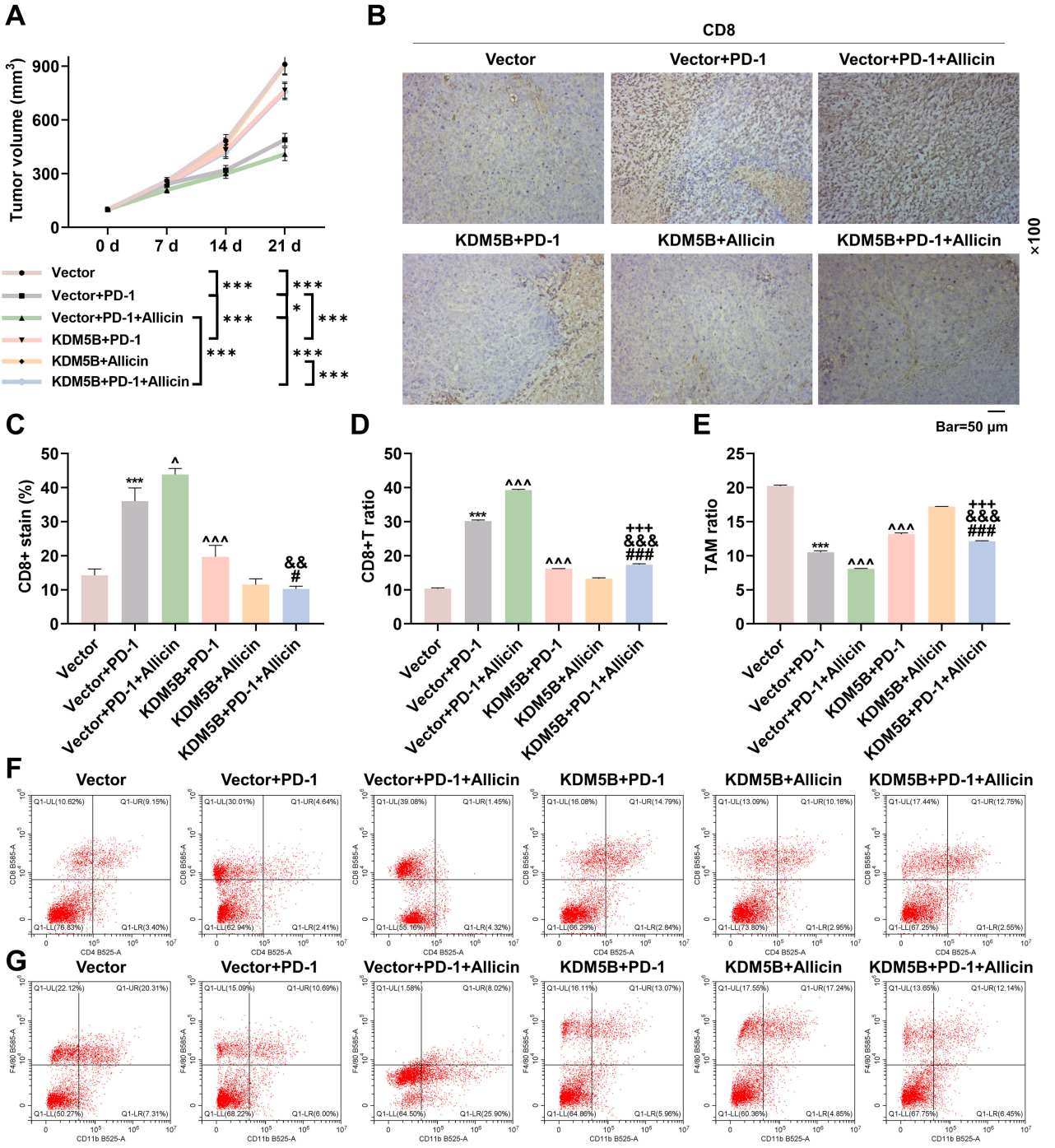

Fig. 7. Allicin enhanced the anti-tumour effect of anti-PD-1 by modulating KDM5B. (A) The effects of anti-PD-1 and allicin on the growth of transplanted tumours were detected by measuring the volume. (B,C) The effects of anti-PD-1 and allicin on CD8 expression in transplanted tumours were determined by immunohistochemical staining. Magnification: 100×. (D–G) The effects of anti-PD-1 and allicin on CD8+ T cells and TAM infiltration in transplanted tumours were examined by flow cytometry. $^{*}p < 0.05$, $^{***}p < 0.001$ vs. Vector; $^{\wedge}p < 0.05$, $^{\wedge\wedge\wedge}p < 0.001$ vs. Vector+PD-1; $^{\#}p < 0.05$, $^{\#\#\#}p < 0.001$ vs. Vector+PD-1+Allicin; $^{\&\&}p < 0.01$, $^{\&\&\&}p < 0.001$ vs. KDM5B+PD-1; $^{+++}p < 0.001$ vs. KDM5B+Allicin. All experiments were repeated three times to average.

necessitating future pharmacokinetic studies to bridge the bench-to-bedside gap. Besides, all current data are derived from cell and mouse models. Clinical relevance needs to be confirmed through patient samples or clinical trials. Secondly, although KDM5B/SETDB1 inhibition is associated with increased CD8+ T cell infiltration, the key chemotactic factor pathway mediating this process requires functional validation. Our experiment did not evaluate the con-

tribution of other immune cells within the tumour (such as TAMs and CAFs) to T cell recruitment, warranting future investigation. Thirdly, this study did not directly assess the functional status of CD8+ T cells (such as IFN-γ secretion and cytotoxic activity). Although increased infiltration is associated with therapeutic effect, functional experiments are needed to confirm its causality. Finally, while A549 and H1299 represented common NSCLC subtypes, other genotypes were not systematically analyzed in this study. Future work should validate our findings in patient-derived organoids or additional cell lines reflecting NSCLC diversity.

Conclusion

In summary, this study demonstrates that allicin may regulate the proliferation of NSCLC cells and tumour growth through inhibition of the KDM5B/SETDB1 signaling axis. *In vivo* experiments reveal synergistic anti-tumour effects when allicin combines with PD-1 antibodies; however, its specific mechanisms, including whether it modulates tumour microenvironment or immune cell functions, require further validation. These findings provide preliminary experimental evidence for exploring allicin's potential applications in tumour immunotherapy, though clinical translation still requires substantial research.

Abbreviations

Allicin-L, mice treated with 3.5 mg/kg of allicin; Allicin-H, mice treated with 7 mg/kg of allicin; ANOVA, analysis of variance; BCA, bicinchoninic acid; BSA, bovine serum albumin; CCK-8, cell counting kit-8; CTLA-4, cytotoxic T-lymphocyte associated antigen 4; DAB, Diaminobenzidine; DEPC, diethyl pyrocarbonate; ECL, enhanced chemiluminescence; FMO, fluorescence minus one; GAPDH, glyceraldehyde-3-phosphate dehydrogenase; H3K9, Histone H3 Lysine 9; H&L, Heavy & Light chains; ICIs, immune checkpoint inhibitors; IgG, Immunoglobulin G; iRAEs, immune-related adverse events; JMJD, Jumonji C domain-containing; KDM5B, lysine demethylase 5B; NC, KDM5B overexpression negative control for plasmid; NSCLC, non-small cell lung cancer; PBS, phosphate buffered saline; PD-1, programmed death receptor 1; PVDF, polyvinylidene fluoride; qRT-PCR, quantitative real-time polymerase chain reaction; SDS-PAGE, sodium dodecyl sulfate polyacrylamide gel electrophoresis; SETDB1, SET domain bifurcated histone lysine methyltransferase 1; shSETDB1, short hairpin RNA for SETDB1; TAM, tumour-associated macrophages. shSETDB1, short hairpin RNA for SETDB1; shNC, negative control for shSETDB1.

Availability of Data and Materials

The analyzed data sets generated during the study are available from the corresponding author on reasonable request.

Author Contributions

CC and WNL designed the research study. CC, WNL, YLJ, GFR, HJY and JF performed the research. YLJ and GFR collected and analyzed the data. CC, WNL and GFR have been involved in drafting the manuscript and all authors have been involved in revising it critically for important intellectual content. All authors gave final approval of the version to be published. All authors have participated sufficiently in the work to take public responsibility for appropriate portions of the content and agreed to be accountable for all aspects of the work in ensuring that questions related to its accuracy or integrity.

Ethics Approval and Consent to Participate

This work was approved by the Ethics Committee of Zhejiang Baiyue Biotech Co., Ltd. for Experimental Animals Welfare (No. ZJBYLA-IACUC-20230915).

Acknowledgment

Not applicable.

Funding

This work was supported by the Hangzhou Health Science and Technology Plan [grant number B20230016].

Conflict of Interest

The authors declare no conflict of interest.

Supplementary Material

Supplementary material associated with this article can be found, in the online version, at https://doi.org/10.24976/Discov.Med.202537201.193.

References

[1] Wang T, Wang Y, Luo Y, Chen H. Longitudinal Study on Changes of Cancer-Related Fatigue in Elderly Patients with Postoperative Chemotherapy for Non-Small Cell Lung Cancer. Annali Italiani Di Chirurgia. 2024; 95: 22–29.

[2] Zheng RS, Chen R, Han BF, Wang SM, Li L, Sun KX, *et al*. Cancer incidence and mortality in China, 2022. Chinese Journal of Oncology. 2024; 46: 221–231. https://doi.org/10.3760/cma.j.cn112152-20240119-00035. (In Chinese)

[3] Bajbouj K, Al-Ali A, Ramakrishnan RK, Saber-Ayad M, Hamid Q. Histone Modification in NSCLC: Molecular Mechanisms and Therapeutic Targets. International Journal of Molecular Sciences. 2021; 22: 11701. https://doi.org/10.3390/ijms222111701.

[4] Alduais Y, Zhang H, Fan F, Chen J, Chen B. Non-small cell lung cancer (NSCLC): A review of risk factors, diagnosis, and treatment. Medicine. 2023; 102: e32899. https://doi.org/10.1097/MD.0000000000032899.

[5] Desai A, Peters S. Immunotherapy-based combinations in metastatic NSCLC. Cancer Treatment Reviews. 2023; 116: 102545. https://doi.org/10.1016/j.ctrv.2023.102545.

[6] Lazzari C, Spagnolo CC, Ciappina G, Di Pietro M, Squeri A, Passalacqua MI, *et al*. Immunotherapy in Early-Stage Non-Small Cell Lung Cancer (NSCLC): Current Evidence and Perspectives. Current Oncology. 2023; 30: 3684–3696. https://doi.org/10.3390/curroncol30040280.

[7] Rui R, Zhou L, He S. Cancer immunotherapies: advances and bottlenecks. Frontiers in Immunology. 2023; 14: 1212476. https://doi.org/10.3389/fimmu.2023.1212476.

[8] Naimi A, Mohammed RN, Raji A, Chupradit S, Yumashev AV, Suksatan W, *et al*. Tumor immunotherapies by immune checkpoint inhibitors (ICIs); the pros and cons. Cell Communication and Signaling. 2022; 20: 44. https://doi.org/10.1186/s12964-022-00854-y.

[9] Tang S, Qin C, Hu H, Liu T, He Y, Guo H, *et al*. Immune Checkpoint Inhibitors in Non-Small Cell Lung Cancer: Progress, Challenges, and Prospects. Cells. 2022; 11: 320. https://doi.org/10.3390/cells11030320.

[10] Yi M, Zheng X, Niu M, Zhu S, Ge H, Wu K. Combination strategies with PD-1/PD-L1 blockade: current advances and future directions. Molecular Cancer. 2022; 21: 28. https://doi.org/10.1186/s12943-021-01489-2.

[11] Pu Y, Ji Q. Tumor-Associated Macrophages Regulate PD-1/PD-L1 Immunosuppression. Frontiers in Immunology. 2022; 13: 874589. https://doi.org/10.3389/fimmu.2022.874589.

[12] Baxi S, Yang A, Gennarelli RL, Khan N, Wang Z, Boyce L, *et al*. Immune-related adverse events for anti-PD-1 and anti-PD-L1 drugs: systematic review and meta-analysis. BMJ (Clinical Research Ed.). 2018; 360: k793. https://doi.org/10.1136/bmj.k793.

[13] Chan JYY, Yuen ACY, Chan RYK, Chan SW. A review of the cardiovascular benefits and antioxidant properties of allicin. Phytotherapy Research. 2013; 27: 637–646. https://doi.org/10.1002/ptr.4796.

[14] Catanzaro E, Canistro D, Pellicioni V, Vivarelli F, Fimognari C. Anticancer potential of allicin: A review. Pharmacological Research. 2022; 177: 106118. https://doi.org/10.1016/j.phrs.2022.106118.

[15] Talib WH, Baban MM, Azzam AO, Issa JJ, Ali AY, AlSuwais AK, *et al*. Allicin and Cancer Hallmarks. Molecules. 2024; 29: 1320. https://doi.org/10.3390/molecules29061320.

[16] Chang Z, An L, He Z, Zhang Y, Li S, Lei M, *et al*. Allicin suppressed *Escherichia coli*-induced urinary tract infections by a novel MALT1/NF-κB pathway. Food & Function. 2022; 13: 3495–3511. https://doi.org/10.1039/d1fo03853b.

[17] Jiang YL, Yu HJ, Zhang NB, Chen C. Mechanism of allicin in enhancing radiosensitivity of non-small cell lung cancer A549 cells via miR-486-5p/KDM5B axis. Journal of Wenzhou Medical University. 2022; 52: 358–364. (In Chinese)

[18] Zhang SM, Cai WL, Liu X, Thakral D, Luo J, Chan LH, *et al*. KDM5B promotes immune evasion by recruiting SETDB1 to silence retroelements. Nature. 2021; 598: 682–687. https://doi.org/10.1038/s41586-021-03994-2.

[19] Fu YD, Huang MJ, Guo JW, You YZ, Liu HM, Huang LH, *et al*. Targeting histone demethylase KDM5B for cancer treatment. European Journal of Medicinal Chemistry. 2020; 208: 112760. https://doi.org/10.1016/j.ejmech.2020.112760.

[20] Markouli M, Strepkos D, Piperi C. Structure, Activity and Function of the SETDB1 Protein Methyltransferase. Life. 2021; 11: 817. https://doi.org/10.3390/life11080817.

[21] Luo F, Lu FT, Cao JX, Ma WJ, Xia ZF, Zhan JH, *et al*. HIF-1α inhibition promotes the efficacy of immune checkpoint blockade in the treatment of non-small cell lung cancer. Cancer Letters. 2022; 531: 39–56. https://doi.org/10.1016/j.canlet.2022.01.027.

[22] Bai X, Cheng Y, Wan H, Li S, Kang X, Guo S. Natural Compound Allicin Containing Thiosulfinate Moieties as Transmembrane Protein 16A (TMEM16A) Ion Channel Inhibitor for Food Adjuvant Therapy of Lung Cancer. Journal of Agricultural and Food Chemistry. 2023; 71: 535–545. https://doi.org/10.1021/acs.jafc.2c06723.

[23] Martins C, Rasbach E, Heppt MV, Singh P, Kulcsar Z, Holzgruber J, *et al*. Tumor cell-intrinsic PD-1 promotes Merkel cell carcinoma growth by activating downstream mTOR-mitochondrial ROS signaling. Science Advances. 2024; 10: eadi2012. https://doi.org/10.1126/sciadv.adi2012.

[24] Lerner EC, Woroniecka KI, D'Anniballe VM, Wilkinson DS, Mohan AA, Lorrey SJ, *et al*. CD8$^+$ T cells maintain killing of MHC-I-negative tumor cells through the NKG2D-NKG2DL axis. Nature Cancer. 2023; 4: 1258–1272. https://doi.org/10.1038/s43018-023-00600-4.

[25] Chen P, Liu Y, Wen Y, Zhou C. Non-small cell lung cancer in China. Cancer Communications. 2022; 42: 937–970. https://doi.org/10.1002/cac2.12359.

[26] de Castro G, Jr, Kudaba I, Wu YL, Lopes G, Kowalski DM, Turna HZ, *et al*. Five-Year Outcomes With Pembrolizumab Versus Chemotherapy as First-Line Therapy in Patients With Non-Small-Cell Lung Cancer and Programmed Death Ligand-1 Tumor Proportion Score $\geq$1% in the KEYNOTE-042 Study. Journal of Clinical Oncology. 2023; 41: 1986–1991. https://doi.org/10.1200/JCO.21.02885.

[27] Daud AI, Wolchok JD, Robert C, Hwu WJ, Weber JS, Ribas A, *et al*. Programmed Death-Ligand 1 Expression and Response to the Anti-Programmed Death 1 Antibody Pembrolizumab in Melanoma. Journal of Clinical Oncology. 2016; 34: 4102–4109. https://doi.org/10.1200/JCO.2016.67.2477.

[28] Stenehjem DD, Tran D, Nkrumah MA, Gupta S. PD1/PDL1 inhibitors for the treatment of advanced urothelial bladder cancer. OncoTargets and Therapy. 2018; 11: 5973–5989. https://doi.org/10.2147/OTT.S135157.

[29] Kuo KT, Huang WC, Bamodu OA, Lee WH, Wang CH, Hsiao M, *et al*. Histone demethylase JARID1B/KDM5B promotes aggressiveness of non-small cell lung cancer and serves as a good prognostic predictor. Clinical Epigenetics. 2018; 10: 107. https://doi.org/10.1186/s13148-018-0533-9.

[30] Zhao Z, Su Z, Liang P, Liu D, Yang S, Wu Y, *et al*. USP38 Couples Histone Ubiquitination and Methylation via KDM5B to Resolve Inflammation. Advanced Science. 2020; 7: 2002680. https://doi.org/10.1002/advs.202002680.

[31] Zhang Y, Gao Y, Jiang Y, Ding Y, Chen H, Xiang Y, *et al*. Histone demethylase KDM5B licenses macrophage-mediated inflammatory responses by repressing Nfkbia transcription. Cell Death and Differentiation. 2023; 30: 1279–1292. https://doi.org/10.1038/s41418-023-01136-x.

[32] Gaillard S, Charasson V, Ribeyre C, Salifou K, Pillaire MJ, Hoffmann JS, *et al*. KDM5A and KDM5B histone-demethylases contribute to HU-induced replication stress response and tolerance. Biology Open. 2021; 10: bio057729. https://doi.org/10.1242/bio.057729.

[33] Pan D, Bao X, Hu M, Jiao M, Li F, Li CY. SETDB1 Restrains Endogenous Retrovirus Expression and Antitumor Immunity during Radiotherapy. Cancer Research. 2022; 82: 2748–2760. https://doi.org/10.1158/0008-5472.CAN-21-3523.

[34] Griffin GK, Wu J, Iracheta-Vellve A, Patti JC, Hsu J, Davis T, *et al*. Epigenetic silencing by SETDB1 suppresses tumour intrinsic immunogenicity. Nature. 2021; 595: 309–314. https://doi.org/10.1038/s41586-021-03520-4.